

# Pulsed vs dc I-V measurements on $\text{Al}_x\text{V}_{1-x}\text{O}_2$ ( $x = 0\text{--}0.013$ ) single crystals: Unmasking a non-thermal electric field effect on these crystals

Cite as: Appl. Phys. Lett. **119**, 221901 (2021); doi: [10.1063/5.0073797](https://doi.org/10.1063/5.0073797)

Submitted: 4 October 2021 · Accepted: 11 November 2021 ·

Published Online: 29 November 2021



View Online



Export Citation



CrossMark

L. Patlagan, I. Taitler, G. M. Reisner, and B. Fisher<sup>a)</sup> 

## AFFILIATIONS

Physics Department, Technion, Haifa 32000, Israel

<sup>a)</sup> Author to whom correspondence should be addressed: [phr06bf@physics.technion.ac.il](mailto:phr06bf@physics.technion.ac.il)

## ABSTRACT

The thermally induced insulator–insulator transition in Al-doped and the insulator–metal transition in doped as well as in pure  $\text{VO}_2$  single crystals are replicated in their dc I-V characteristics due to self-heating. In the investigation reported herein, self-heating (a lattice effect) was totally or almost totally avoided by using current pulses of millisecond durations, thus leaving the stage for electron heating. At low currents, the pulsed I-V are close to, or perfectly Ohmic, corresponding to the room temperature value of the resistance. Above a threshold, the voltage jumped backward and the current upward, marking a finite drop in resistance by 12%–24% for the different crystals; from there on, the resistance decreased linearly with the increasing voltage. Most R(V) traces were reproducible with small hysteresis upon increasing and decreasing currents. This behavior suggests an insulator-mixed-metal-insulator transition with metallic domains increasing with the increasing voltage (current). No reproducible behavior of the pulsed I-V characteristic of Al-doped crystals suggests onset of a non-thermal insulator–insulator transition. The interesting question now is what is the true nature of the material under the high pulsed voltage.

Published under an exclusive license by AIP Publishing. <https://doi.org/10.1063/5.0073797>

Non-linear electrical conductivity of resistive materials and related effects may be of electronic origin or a self-heating effect, the latter leading mostly to artifacts. Over several years, when striking non-linear conductivity effects, measured with dc, were interpreted in terms of electronic effects, I-V characteristics obtained using a pulse generator and a memory scope were very efficient in discriminating between simple facts and dramatic artifacts.<sup>1,2</sup> The dc  $I(V)$  of these resistive materials exhibited at high currents a current-controlled negative-differential-resistance (CCNDR) and hysteresis, which masked a perfectly Ohmic or a moderately non-Ohmic conductivity obtained by pulsed measurements. Nevertheless, phenomena induced by self-heating may be fascinating, provided that they are properly identified. The most impressive effect is the self-heating induced resistive-switching in phase-change oxides of which  $\text{VO}_2$  is the prototype material. This material is famous for its steep resistance jump of five orders of magnitude (in four probe measurements on pure single crystals) upon the thermally induced insulator to metal transition (IMT); it is associated with a structural phase transition from the insulating monoclinic (M1) to metallic rutile (R) structure, and with a significant change in its optical properties, that occur above, but close to room temperature ( $T_{\text{IMT}} = 340\text{ K}$ ). Unlike the case of external heating,

which leads to full IMT, self-heating does not lead to a full transition to the metallic state, because the low power developed in the metal cannot cover the losses at  $T_{\text{IMT}}$ . Instead, a mixed metal–insulator state sets in. Tracing dc I-V characteristics of  $\text{VO}_2$  single crystals under the microscope reveals a wealth of static and dynamic metal–insulator domain patterns<sup>3–5</sup> of which the narrow insulating domain sliding within the metallic background in the sense of the electric current with velocity determined by exchange of Peltier heat with latent heat is the most remarkable. Although the dominant role of Joule heating in the resistance switching of single crystals, nanowires, and films of  $\text{VO}_2$  was recognized for a long time,<sup>3–6</sup> the anticipated advantages of non-thermal insulator–metal switching in this material have initiated intense research in this field. The resolution of this issue was recently reached in heavily doped  $\text{VO}_2$  (and  $\text{V}_2\text{O}_3$ ) nanowires;<sup>7</sup> in such samples, relatively low electric fields can de-trap large numbers of charge carriers that induce the IMT.

For a range of concentrations, Al-doped single crystals are triclinic (T) and insulating at room temperature (RT) and exhibit a thermally induced transition to the insulating monoclinic M2 phase at temperatures above RT and below  $T_{\text{IMT}}$ .<sup>8–10</sup> The resistance jump at the  $T \rightarrow \text{M2}$  transition is by a factor of up to 2. While the M2 to R

transition is strongly first order with latent heat similar to the  $M1 \rightarrow R$  transition, the  $T \rightarrow M2$  transition is a weak first order transition with a much lower latent heat that decreases with an increase in doping.<sup>11</sup> The thermally induced insulator–insulator–transition (IIT) in Al-doped  $\text{VO}_2$  single crystals and the opposite transition upon cooling were replicated in the dc I-V characteristics of the crystals upon increasing and decreasing currents.<sup>12</sup> The nucleation of embedded phases (M2 within T and R within M2), their expansion with the increase in current, and contraction with the decrease in current were visualized in several Al doped samples; no sliding domains were observed in this system due to the much lower Peltier coefficient in doped crystals (see the [supplementary material](#)). A voltage-controlled NDR (VCNDR) represents the resistance jump in the I-V characteristics. The stability conditions for CCNDR and VCNDR (lack of switching) are contradictory, that is, while a voltage source is ideal for tracing the first one, a current source is ideal for tracing the second. As shown in Ref. 12, the replication of the IIT in the I-V characteristics is highly reproducible as long as the current does not exceed the onset of the insulator–mixed-metal–insulator–transition (ImMIT): Switching in the CCNDR regime under large deviations from steady state conditions may cause damage or disorder in the crystal. Nevertheless, small deviations from the steady state that enhance steep switching are beneficial because they leave visible marks upon the onset of the transitions on the I-V traces.

The present pulsed measurements represent an attempt to unmask possible non-thermal IIT in Al-doped  $\text{VO}_2$  and non-thermal ImMIT in both Al-doped and in pure  $\text{VO}_2$  single crystals.

The crystals used in this investigation were chosen from the batches of crystals used in our recent investigations (see Ref. 5 for pure  $\text{VO}_2$  crystals and Ref. 12 for the Al-doped crystal).

$I(V)$  and  $R(T)$  of the crystals were measured in the two-probe configurations (with connected adjacent voltage and current probes). The contacts were indium–amalgam dots. These are Ohmic contacts of low resistance for insulating (semiconducting)  $\text{VO}_2$ . With these contacts, the samples are free to move, being held only by surface tension. dc and pulsed I-V measurements were carried out at ambient temperature ( $25^\circ\text{C}$ ); the dc I-V loops were recorded on a YEW type 3036 X-Y recorder; the pulsed  $I(V)$  measurements were carried out using a Keithley 237 source and a Keysight DSOX 2002 oscilloscope (see Fig. 1). The RT Ohmic resistances of the crystals chosen for the present investigation were in the range of 10–100 k $\Omega$  in order to reduce as much as possible the rise time of the pulses, corresponding to far thicker and less robust crystals than those used in the past.<sup>5,12</sup>

The protocol of the investigation, which included 5 or more stages for the Al-doped  $\text{VO}_2$  crystals, was planned so as to protect the fragile crystals from damage; dc measurements were often stopped prior to ImMIT, then followed by  $R(T)$  up to IMT, and then repeated to include IMT. In spite of all the precautions, some degree of damage/disorder could not be avoided and a significant number of crystals were lost during the various stages of the measurements.

The typical behavior of voltage as function of time for short (1 ms) and long (100 ms) pulses applied to one of our crystals in series with the test resistor are shown in Fig. 1. After a finite rise time of  $\sim 0.2$  ms  $V_1$  is constant with time; a small overshoot is superimposed on the rise time of the total voltage ( $V_2$ ), which is constant for the second half of the pulse.  $V_1$  is constant over all the duration of the long

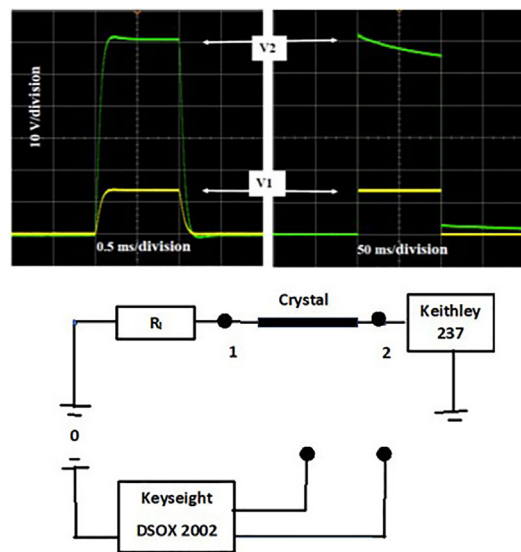


**FIG. 1.** The circuit for the pulsed measurements (bottom) and an example of two pulses, one of the 1 ms duration (left) and the second of a 100 ms duration (right) showing the effect of Joule heating. The pulses shown here were applied on crystal  $\text{Al}_{0.01}\text{V}_{0.99}\text{O}_2$  (3b) (see below).  $R_1$  is used as a test resistor.

pulse (100 ms), while  $V_2$  decreases with time due to Joule heating of the crystal.

The pulsed and dc I-V of three crystals of different compositions and their resistances  $R$  as function of  $V$  derived from  $I(V)$  are presented in the text.  $R(T)$  for all investigated crystals, I-V characteristics, and  $R(V)$  for additional crystals are presented in the [supplementary material](#). The main properties of all the investigated crystals and the main results for all are summarized in Table I.

The quality of the  $\text{VO}_2$  crystal D2(4) chosen for this investigation may be evaluated by its activation energy  $\Delta$  ( $=0.40$  eV) and narrow hysteresis obtained from the Arrhenius plot of its resistance shown in the [supplementary material](#), Fig. 1. This  $\Delta$  is not far from the highest values cited in the literature for pure  $\text{VO}_2$  crystals, 0.45–0.46 eV (see Refs. 5 and 13). The dc  $I(V)$  in Fig. 2(a) is typical for non-linear conductivity of pure  $\text{VO}_2$  single crystals induced by self-heating, leading at high currents to CCNDR, which is followed by the onset of ImMIT [see red arrow in (a)]. The rather large difference between the trace of increasing and decreasing currents is the penalty for choosing a thick sample. In samples with cross sections smaller by  $\sim$ two orders of magnitude, the traces for increasing and decreasing currents practically coincide (see, e.g., Fig. 1 in Ref. 5). The  $I(V)$  trace obtained with 1 ms duration current pulses deviates slightly from the Ohmic trace and exhibits a sudden jump to a trace with a higher slope. Figure 2(b) shows  $R$  ( $=V/I$ ) from the data taken from (a), plotted vs  $V$ . The  $R(V)$  trace shows a weak non-ohmicity at low  $V$  but tends to reach the RT Ohmic dc value with an increase in  $V$ . Around 50 V, the trace jumps to a lower resistance and lower voltage; the drop of resistance exceeds 20%; this jump is followed by a linear decrease in  $R$  with an increase in  $V$ . This pulsed  $R(V)$  trace is almost perfectly reproduced on its way back, upon decreasing current/voltage except for a narrow hysteresis. This seems somewhat analogous to the transition to the mMI state induced by self-heating; there, the decreasing resistance with the

**TABLE I.** Crystal dimensions, activation energies  $\Delta$ , of the three insulating phases, M1, T, and M2, voltage at jump ( $V_j$ ), relative change in resistance at jump  $\Delta R/R_j$  and  $V(R=0)$  from the linear fit of  $R(V)$ .

Sample	Dimensions $w \times h \times l$ (cm <sup>3</sup> )	$\Delta$ (M1) (eV)	$\Delta$ (T) (eV)	$\Delta$ (M2) (eV)	$V_j$ (V)	$\Delta R/R_j$	$V(R=0)$ (V)	$R^2$
VO <sub>2</sub> [D2(4)]	0.049 × 0.012 × 0.075	0.40			50	−0.23	280	0.715
Al <sub>0.007</sub> V <sub>0.993</sub> O <sub>2</sub> (8)	0.041 × 0.032 × 0.075		0.32↑ 0.35↓	0.35	25	−0.12	686	0.594
Al <sub>0.01</sub> V <sub>0.99</sub> O <sub>2</sub> (3b)	0.033 × 0.017 × 0.075		0.26	0.27	40	−0.16	360	0.747
Al <sub>0.007</sub> V <sub>0.993</sub> O <sub>2</sub> (6)	0.022 × 0.025 × 0.075		0.21	0.23	NA	NA	NA	NA
Al <sub>0.007</sub> V <sub>0.993</sub> O <sub>2</sub> (7)	0.024 × 0.014 × 0.075		0.28	0.27	26	−0.12	480	0.906
Al <sub>0.013</sub> V <sub>0.987</sub> O <sub>2</sub> (3)	0.045 × 0.024 × 0.075		0.26	0.28	...	...	...	...
Split of crystal	0.024 × 0.010 × 0.075		0.25	0.34	50	−0.24	373	0.648

increasing current [decreasing voltage in the NDR regime, see, e.g., the bottom of 2(b)] is due to the increasing size/numbers of metallic domains that cross the widths of the crystals and have been visualized many times (see, e.g., Ref. 5). Large current jumps in I-V measurements across the widths of thin VO<sub>2</sub> films, far below  $T_{\text{IMT}}$ , were reported in Ref. 14 and attributed to electrically triggered insulator-metal-transition (E-IMT).

In the following figures, results for Al-doped samples are presented. Their activation energies in the triclinic and M2 insulating phases obtained from Arrhenius plots are presented in the [supplementary material](#), Fig. 1; they fall within the values obtained before.<sup>12</sup>

The dc and pulsed I-V characteristics of the Al<sub>0.007</sub>V<sub>0.993</sub>O<sub>2</sub> (8) single crystal are presented in Fig. 3(a). It shows the T → M2 transition

upon increasing dc current and the opposite transition upon decreasing dc current. Being aware of the sensitivity of the Al-doped crystals, the dc ImMIT was not included within the range of measurements. At low V, the deviation of pulsed R(V) from the Ohmic dc RT value is small. Here too, the small change in pulsed R(V) over a wide range of voltage is in strong contrast to the large change of the dc R(V) over a narrow range of voltage. The previous scenario is repeated in this crystal too: at a threshold voltage of ~25 V, R(V) exhibits a jump of about 12% to a lower value followed by a linear decrease with an increase in V. The interpretation of the downwards jump of R(V) in terms of the appearance of a metallic domain and the appearance of larger metallic domains for pulses of higher voltages is simpler for this specific composition. In pure single crystals, the scenario may be complicated by the dynamic nature of the domain patterns. The visualization of the mixed state of a VO<sub>2</sub> crystal doped with 0.7% Al shows the expansion or contraction of the embedded phase upon increasing or decreasing currents (see Fig. 5 of Ref. 12 and cover page of the issue). The IIT, though visible on the dc traces, leaves no mark on the pulsed trace.

The results of the pulsed and dc I-V measurements for the Al<sub>0.01</sub>V<sub>0.99</sub>O<sub>2</sub> (3b) single crystal presented in Fig. 4 are the simplest and most straightforward of this investigation. The T → M2 transition at currents below the onset of CCNDR, the IMT above it (see black and red arrows, respectively), and their opposite transitions (see blue and black arrows, respectively) are well separated on this trace. The Ohmic nature of the pulsed measurements at low voltages is further emphasized in (b) by the lack of any dependence of R on V up to the jump followed by a linear decrease in R on V. The constant resistance at low V shows that the jump occurs at RT. Here again, the IIT upon increasing and decreasing currents leaves no visible mark on the pulsed I-V and, thus, on the R(V) traces. The trace of the 1 ms pulse at the left of Fig. 1 ( $V_2 = 60$  V,  $V_1 = 13.5$  V and  $I = 1.7$  mA) was recorded at the end of the corresponding pulsed I-V traced in Fig. 4(a); the trace of the 100 ms pulse for same current shows the effect of Joule heating: V2 decreases gradually with time. The voltage on the test (power) resistor, V1, is constant over this time.

The crystal with the higher Al concentration, Al<sub>0.013</sub>V<sub>0.987</sub>O<sub>2</sub> (3), was thick with relatively low resistance. The careful protocol applied to the measurements on this crystal did not prevent its splitting along its length, the rutile c-axis, at a rather advanced stage of measurements. A thin split of the crystal with high resistance could be used for further measurements. The detailed results of measurements on the initial crystal and on the split are presented in the [supplementary material](#), Fig. 4. The results (primarily for the split) are presented in Table I.

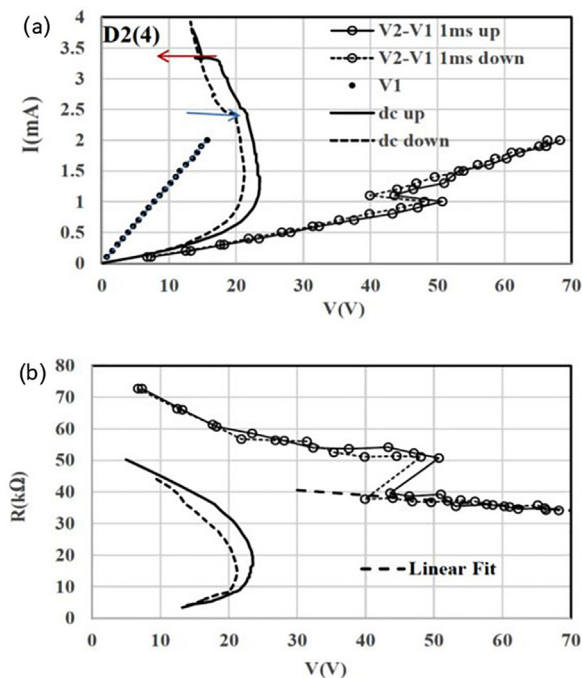


**FIG. 2.** (a) Pulsed I-V and dc loops of a pure VO<sub>2</sub> single crystal labeled D2(4). (b)  $R(V) = (V_2 - V_1)/I$  taken from (a). Note the sudden drop by ~20% in R measured by pulses. The arrows in (a) mark the I → mMI switching (red) and the opposite switching (blue) along the load line ( $R_L = 100$  kΩ).

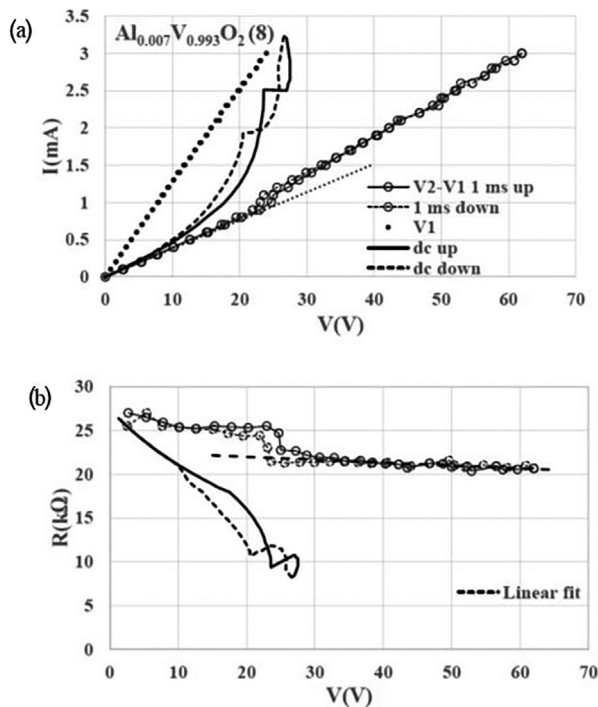


**FIG. 3.** (a) Pulsed I-V traces and dc loop of  $\text{Al}_{0.007}\text{V}_{0.993}\text{O}_2$  (8) single crystal. (b)  $R(V) [= (V_2 - V_1)/I]$  taken from (a). Note the sudden drop by  $\sim 12\%$  in  $R(V)$  taken from (a).

The main results obtained in this work are shown in Table I. The sudden decrease in the resistance of the different crystals occurs at  $V_j \leq 50$  V corresponding to electric fields  $E \leq 670$  V/cm on our 0.075 cm long samples, far lower than the threshold for de-trapping of electrons from impurities and inducing the IMT reported in Ref. 7; this indicates that if de-trapping is involved in this switching event, it is limited to a narrow volume, possibly causing nucleation. The data of the resistance after jump as function of voltage for all investigated crystals are plotted vs  $V$  in the [supplementary material](#), Fig. 5, with fitted linear trendlines. Remarkably, the relative slope of the trend-line for the undoped crystal D2(4) is highest. The inverse of the relative slopes yields the extrapolated values of  $V(R=0)$  shown in Table I (see second before last column); it ranges between 280 and 686 V, corresponding to  $\sim 4000$ – $9000$  V/cm far closer to the threshold found in Ref. 7. The most striking result is that  $V(R=0)$  for  $\text{VO}_2$  [D2(4)] is the lowest. This shows that in the present case, an additional factor to de-trapping of charge carriers inducing E-IMT must play an important role; the effect of a lower concentration of impurities in the pure  $\text{VO}_2$  crystal is probably compensated by the higher energy flux density accompanying the electronic current density in the insulator— $\Pi J$ , where  $\Pi$  is the Peltier coefficient of the insulator–metal couple and  $J$  is the current density<sup>3</sup> (see paragraphs devoted to this issue in the [supplementary material](#)).

In summary, dc and pulsed I-V measurements were carried out on pure and Al doped single crystals, the latter exhibiting a thermally induced insulator–insulator transition above RT and below  $T_{\text{IMT}}$ . This investigation was aimed at revealing non-thermal effects of the electric

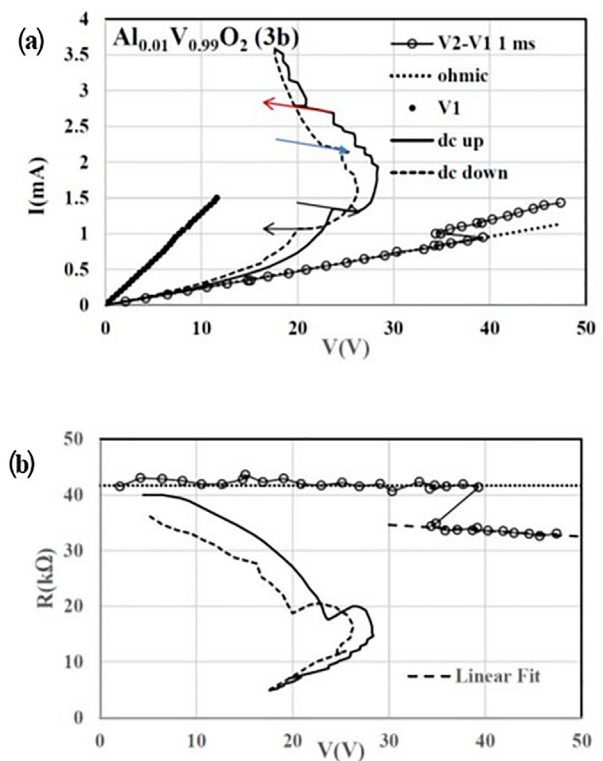


**FIG. 4.** (a) Pulsed I-V trace and dc loop of the  $\text{Al}_{0.01}\text{V}_{0.99}\text{O}_2$  (3b) single crystal. (b)  $R(V) [= (V_2 - V_1)/I]$  taken from (a). Note the constant  $R(V)$  up to its sudden drop by  $\sim 20\%$  in  $R(V)$  followed by a linear decrease with an increase in  $V$ . The arrows in (a) mark the  $I \rightarrow \text{mMI}$  switching (red) and the opposite switching (blue) along the load line ( $R_L = 100$  k $\Omega$ ). The black arrows in (a) mark the  $T \rightarrow \text{M2}$  and the  $\text{M2} \rightarrow T$  transitions upon increasing and decreasing currents, respectively.

field on the transitions, usually masked by Joule heating. The pulsed measurements for crystals, doped and undoped, reveal a jump that may be attributed to a pure field effect related to the ImMIT. With the increase in the pulsed voltage, the magnitude of the jumps increased, consistent with the decrease in resistance. The reproducibility of the results and the small hysteresis show that the material during most of the duration of the pulses after the jump is stable, the stability reached on an electronic timescale shorter than milliseconds. This behavior is consistent with the appearance of a metallic domain after the first jump and increasing metallic domains for increasing applied pulses. These domains might be detected by fast optical measurements simultaneously with the applied voltage pulses, provided that these can be applied without heating the samples. If this model is valid, the immediate question is related to the structure of the material: Is the metallic domain monoclinic (M1) or triclinic (T) (without structural transition being involved)?<sup>15,16</sup> On the basis of the present results, we plan to expand this work to include doped  $\text{VO}_2$  single crystals and also to higher ambient temperatures.

See the [supplementary material](#) for Arrhenius plots for all the investigated crystals in this work, I-V characteristics, and  $R(V)$  for single crystals  $\text{Al}_{0.007}\text{V}_{0.993}\text{O}_2$  (6),  $\text{Al}_{0.007}\text{V}_{0.993}\text{O}_2$  (7),  $\text{Al}_{0.013}\text{V}_{0.987}\text{O}_2$  (3),



and its split are presented in the [supplementary material](#). Also, we added a short discussion on the Seebeck coefficient and the Peltier effect.

The authors are indebted to Engineer Idan Sthzeglowski, for his outstanding professional assistance in assembling the measuring system.

## AUTHOR DECLARATIONS

### Conflict of Interest

The Authors declare that there is no conflict of interest.

### DATA AVAILABILITY

The data that support the findings of this study are available within the article and its [supplementary material](#).

## REFERENCES

- <sup>1</sup>B. Fisher, J. Genossar, L. Patlagan, K. B. Chashka, and G. M. Reisner, *Appl. Phys. Lett.* **88**, 152103 (2006).
- <sup>2</sup>B. Fisher, J. Genossar, L. Patlagan, and G. M. Reisner, *EPJ Web Conf.* **40**, 15009 (2013) and references therein.
- <sup>3</sup>B. Fisher, *J. Phys. C* **9**, 1201 (1976).
- <sup>4</sup>Q. Gu, A. Falk, J. Wu, L. Ouyang, and H. Park, *Nano Lett.* **7**, 363 (2007).
- <sup>5</sup>B. Fisher, L. Kornblum, L. Patlagan, and G. M. Reisner, *Phys. Status Solidi B* **257**, 2000074 (2020).
- <sup>6</sup>A. Zimmers, L. Aigouy, M. Mortier, A. Sharoni, S. Wang, K. G. West, J. G. Ramirez, and I. K. Schuller, *Phys. Rev. Lett.* **110**, 056601 (2013).
- <sup>7</sup>Y. Kalcheim, A. Camjayi, J. Del Valle, P. Salev, M. Rozenberg, and I. K. Schuller, *Nat. Commun.* **11**, 2985 (2020).
- <sup>8</sup>G. Villeneuve, M. Drillon, J. C. Launay, E. Marquestaut, and P. Hagenmuller, *Solid State Commun.* **17**, 657 (1975).
- <sup>9</sup>G. Villeneuve, M. Drillon, P. Hagenmuller, M. Nygren, J. P. Pouget, F. Carmona, and P. Delhaes, *J. Phys. C* **10**, 3621 (1977).
- <sup>10</sup>M. Ghedira, H. Vincent, M. Marezio, and J. C. Launay, *J. Sol. State Chem.* **22**, 423 (1977).
- <sup>11</sup>J. P. Pouget, H. Launois, T. M. Rice, P. Dernier, A. Gossard, G. Villeneuve, and P. Hagenmuller, *Phys. Rev. B* **10**, 1801 (1974).
- <sup>12</sup>B. Fisher, L. Patlagan, A. Eyal, and G. M. Reisner, *Phys. Status Solidi A* **218**, 2000820 (2021).
- <sup>13</sup>A. Zylbersztein and N. F. Mott, *Phys. Rev. B* **11**, 4383 (1975).
- <sup>14</sup>Z. Yang, S. Hart, C. Ko, A. Yacoby, and S. Ramanathan, *J. Appl. Phys.* **110**, 033725 (2011).
- <sup>15</sup>V. R. Morrison, R. P. Chatelain, K. L. Tiwari, A. Hendaoui, A. Bruhacs, M. Chaker, and B. J. Siwick, *Science* **346**, 445 (2014).
- <sup>16</sup>L. Vidas, D. Schick, E. Martínez *et al.*, *Phys. Rev. X* **10**, 031047 (2020).